Preprints of the 2012 20th Mediterranean Conference on Control & Automation (MED), Barcelona, Spain, July 3-6, 2012

Basic Control Concept for a Speed-variable Wind Energy Converter in a Low-Power Grid

Prof. Dr.-Ing. Constantinos Sourkounis, *Member, IEEE*
Research Group for Power Systems Technology and Power Mechatronics
Faculty of Electrical Engineering and Information Science, Ruhr-University Bochum
sourkounis@eele.rub.de

Abstract— In order to achieve an high penetration in the electrical grid and an economical utilization of wind energy earlier it is advisable to reduce the pollution on the one hand and to increase the efficiency of wind energy converters on the other. Therefore a new generator system control was design and tested on a 22 kW wind energy converter test bed. The basic control concept is characterised by sufficiently high control dynamics. Besides sufficiently high control reserves for an operation within a broad speed range and high control dynamics, a stable operation over the whole speed range has been obtained.

I. Introduction

At many places, the use of wind energy is confined by the connecting conditions dictated by the electrical grid. Particularly in low-power grid sections, the maximal installable power of the wind energy converter is considerably reduced by the anticipated mains pollutions. In order to avoid an expansion of the electrical grid and achieve an economical utilization of wind energy earlier it is advisable to use low-pollution and efficient wind energy converters [1], [5], [8].

Considering the general requirements on the operation behavior of wind energy converters a novel multi-variable generator system control was design and tested on a 22 kW wind energy converter test bed. The new basic control structure has been particularly designed to make use of wind energy at remote places with excellent wind conditions. For low-power grids, a safe and interruption-free operation must be guaranteed at maximal energy outputs. This requires a control concept which provides sufficient control reserves on the one hand and features a constant behaviour at considerably fluctuating system parameters on the other.

II. Basic Control Concept

Besides the main requirement for operation at maximal possible power variable c_{Pmax}, the control concept to be developed shall meet a number of further requirements. An operation at maximal power variable within a wide range of wind speeds as possible demands, for example, for a stable control over a wide speed range. Since the parameters of the controlled system strongly depend on the speed in this case, a paremeter-insensitive control concept is needed. Moreover, part of the following requirements arise because of the operation of the wind energy converter in a low-power grid:

- Current beats in the DC-link shall be damped as far as possible
- Limitations of the mechanic-electrical energy converter system prescribed by the design parameters must not be exceeded.
- Reactions to the grid or the drive train respectively due to control processes shall be as low as possible.
- Reactive power input from the grid shall be as low as possible and kept constant over the entire operating range.
- Sufficiently high control dynamics shall be achieved.

An energy converter system which offers the possibilities to reach an operating behaviour which takes into account these relevant requirements can be realized by means of a " frequency inverter generator system". In this case, a synchronous machine is connected to the electrical grid by a DC-link converter (see Fig. 1). In the meantime, different models of this energy converter concept are successfully used by a number of wind energy converter manufacturers. Differences relate to the kind of synchronous machine and inverter type.

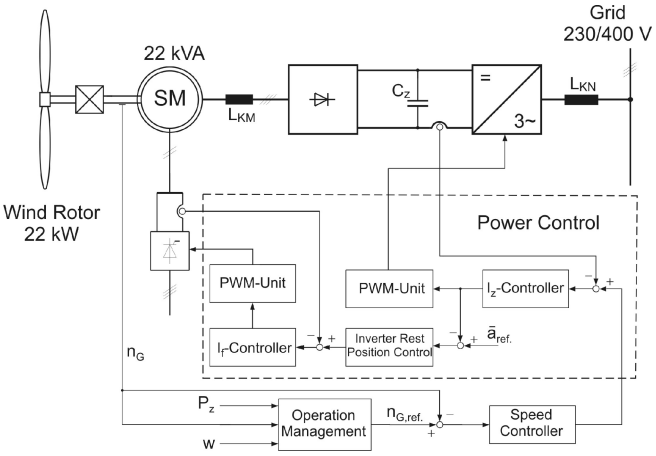

Fig. 1 Principle of the experimental plant

The inverter plays an important role for the operating behaviour of the wind energy converter. For the investigations a converter with uncontrolled rectifier on the generator side and self-commutated inverter on the grid side is assumed. Besides different advantages with regard to loads by harmonic components and reactive power of the electrical grid, it also offers high control dynamic, a fact which is of essential importance in this case. The integration of the self-commutated inverter in the control circuit as a control element can only be realized by means of the control factor A_{wr}. For this purpose, the self-commutated inverter offers a number of more degrees of freedom. Degree of modulation, frequency and phase angle between current and voltage are available as manipulated variables, whereby the frequency must be kept constant and

978-1-4673-2529-5/12/$31.00 ©2012 IEEE

synchronous to the one of the grid when operating in a public grid.

In consideration of the mentioned requirements a control structure has been designed as shown in Fig. 1 which influences the controlled system by two manipulated variables A_{Wr} and I_f. By using the inverter as a actuating element, high control dynamics are achieved. This is particularly important for power limitation in the full-load range [1].

A change of the control factor A_{wr} results in a proportional direct voltage alteration and thus in an alteration of the DC-link current. For the generator this means a change of the current amount but no considerable change of the phase angle $\varphi_{sM} \approx \alpha_u/2$, so that the DC-link current control for the generator works like an active current control. Hereby a complicated control structure is avoided which would become necessary when using the rectifier as actuating element (inverter) for the active power control on the generator side (α_{Gr} = konst. = 0).

The realization current resp. power control by the control factor A_{wr} means for the grid side, the phase angle is available for the adjustment of cosφ parameters (cosφ = 1). This avoids reactive power loads on the one hand and provides a high degree of efficiency for the inverter on the other. The transferred effective power complies with the nominal apparent power.

By increasing the control factor, the first harmonic amplitude of the inverter voltage $\underline{U}_{1Wr}$ is increased, the current flow in the grid rises too. After a dynamic control process, the excitation of the synchronous machine is tracked so that the control factor is reset to its so called "rest position". Therefore the amplitude of manipulated variable of the inverter is fully available for both directions during the next fluctuation of the available primary power.

Operational description and conducted tests prove that the control concept is suitable for both line-commutated and self-commutated inverters without considerable changes.

Due to the wide control range of the excitation current $(0{,}3...2)I_{f,0}$, a dynamic power control can be realized for both converter systems over a broad speed range (e.g. 0,6 to 1,2 fn/p). At the same time, the storage properties of the rotating masses can be used to smooth short-term wind power fluctuations because of the speed-variable operation, so that torque oscillations in the mechanical drive train as well as fluctuations of the elctrical power output are avoided.

This control concept is particularly suitable for synchronous generators with "rotating", uncontrolled rectifier in the excitation circuit where a three-phase controller is used as control element. Achievable control dynamics of the excitation circuit are lower there than in the case of the slip-ring synchronous machine under consideration and it is also unsymmetrically regarding re- and demagnatisation of the rotor because of the freewheeling effect.

III. System analyses of the controlled system

In the following, a detailed description of the control structure is given and approaches made towards a new layout method on the basis of an energy converter system with line-commutated inverter which avoids extensive and complex control structures despite of time-variant parameters and a quite complex system structure. In order to realize an optimal power control, the transfer behaviour of the mechanical-electric energy converter system must be examined at first. Aim is to obtain a simple mathematic model of the controlled system which features sufficient exactness. This is a condition for the application of efficient mathematic methods of controller synthesis.

The system under review can be split into a mechanical and an electrical subsystem. The mechanical subsystem is reduced to a two-mass oscillator for simplification. The mass of the gearbox is hereby added to that of the generator. In order to obtain a model which is as accurately as possible for the more complex electrical subsystem at maintainable efforts, two different approaches have been combined. On the one hand, an analytical examination is carried out since system-relevant equations are known, on the other hand it is possible to identify parameters of the controlled system experimentally on the test facility.

On the basis of the equation system described in the literature [2], [3], the transfer behaviour can be described almost exactly. However, this equation system is much too extensive and therefore unsuitable for modelling a clear controlled system, so that the model has to be simplified specifically.

The block diagram (fig. 2) of the linearised electrical controlled path shows that the two input quantities ($u_{st,f}$, $A_{Wr} \doteq u_{st,wr}$) are dynamically coupled with the two output quantities (i_z, i_f) both stationary and dynamically. For this reason it would be of advantage to represent the electric controlled system in a canonic form for control engineering considerations. The following linear approach has been made:

$$\Delta i_z = G_{11}\Delta u_{st,Wr} + G_{12}\Delta u_{st,f}$$
$$\Delta i_f = G_{21}\Delta u_{st,Wr} + G_{22}\Delta u_{st,f} \qquad (1)$$

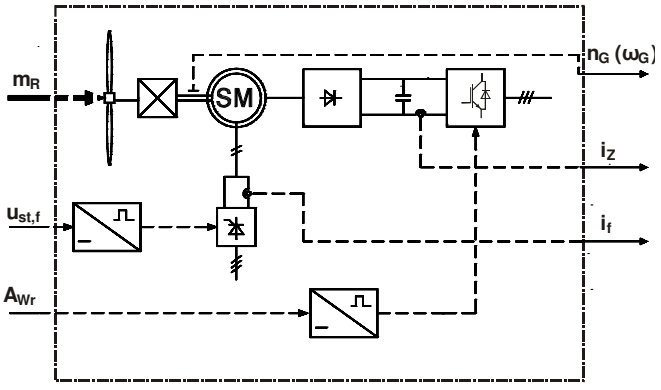

Fig. 2 Controlled system, defined by input and output parameters

The transfer functions of the respective coupling branches are determined on the basis of the equation system of the controlled electrical system. Hereby it is useful for the controller layout to simplify the transfer functions as far as possible, i.e. to only consider the dominant pole and zero points. Since the used method of identification [1] is only applicable to second-order transfer functions at the most, too, two pole points and one zero points at the most should be taken into

consideration for every transfer function in the theoretical analysis , as far as it seems admissible. From the equation system of the controlled electrical system following transfer functions are derived:

$$G_{11} = \frac{K_{11}(1+pT_f)(1+pT_{ce})}{(1+pT_{gr})(1+pT_{kl})}$$

$$G_{12} = \frac{K_{12}(1+pT_S)}{(1+pT_{gr})(1+pT_{kl})} \qquad (2)$$

$$G_{21} = \frac{pT_D}{(1+pT_{gr})(1+pT_{kl})}$$

$$G_{22} = \frac{K_{22}(1+pT^*_{gr})(1+pT^*_{kl})}{(1+pT_{gr})(1+pT_{kl})(1+pT_f)} \quad .$$

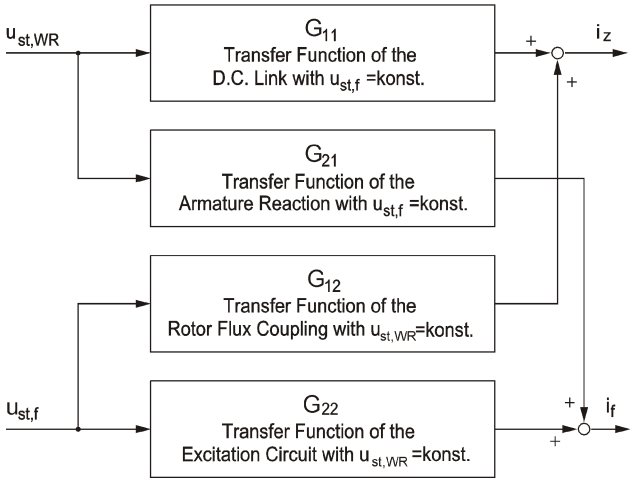

Fig. 3 Block diagram of the two-variables system

The experimental system identification proved that some further simplifications are admissible [1]. The zero point with time constant Ts can be neglected as compared to the dominating poles ($-1/T_{gr}$, $-1/T_{kl}$). At G_{22}, zero point $-1/T_{gr}^*$ is almost compensated by pole $-1/T_f$ as well as zero point $-1/T_{kl}^*$ by pole $-1/T_{kl}$. Therefore the following simplified model emerged for the controlled electric system:

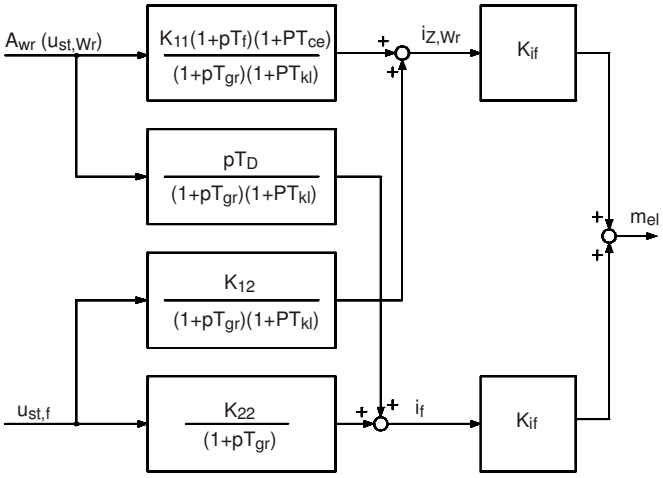

Fig. 4 Resultant global model of the controlled electric system

IV. Controller Synthesis

The developed model of the controlled system is the basis for a parameter optimisation of the described control circuit structure. Fig. 1 shows that the control concept features a double cascaded structure. It is the form of a"two variables control" where two subordinate control cascades (i_f-, i_z-control) are coupled with each other by the structure of the control systems.

A. Controller synthesis for the internal two-variables control

In this section, the parameters for the DC-link (R_{11}) and excitation current controllers (R_{22}) will be determined.

Usual optimization criteria in electrical drive engineering like absolute-value optimum or symmetrical optimum can not simply be applied in this case, since the controlled systems also contain derivative elements in addition to proportional elements and delay elements which have a considerable influence on the system behaviour. This is a result of the intermeshing of the controlled system. Moreover, this intermeshing leads to parallel system sections in addition to the main coupling systems G_{11} and G_{22} respectively for the two controllers R_{11} and R_{22}. Each controller works therefore on a controlled system, the transfer function of which is also co-determined by the parameters of the respective other controller. Fig. 5 shows the manipulation of the controlled system for the DC-link current controller R_{11} by the controller for the excitation current R_{22}.

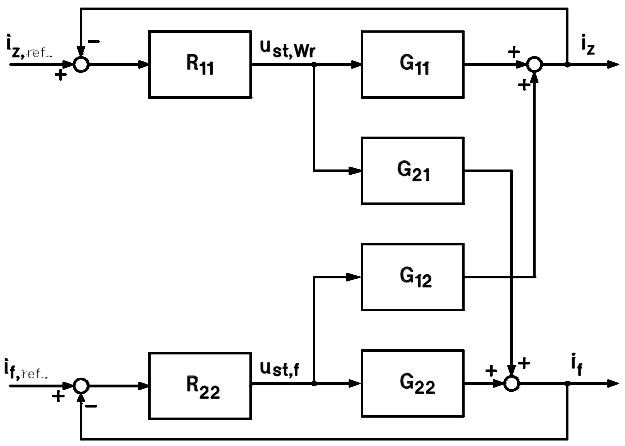

Fig. 5 Internal two-variables control

Therefore the following transfer function of the controlled system results for the DC link current controller:

$$G_{11}^* = G_{11}\left(1 - \frac{G_{21}G_{12}}{G_{22}G_{11}}\,\frac{R_{22}G_{22}}{(1+R_{22}G_{22})}\right) \quad . \qquad (3)$$

Because of the coupling of the two controlled systems, the following procedure has been proposed bearing in mind a controller layout which would be as simple as possible:

- The layout of both controllers has only taken into account the main systems (G_{11}, G_{22})
- The layout under consideration of the zero points was made in such that the reference transfer functions of the non-coupled circuits received a dominant pole pair. In

addition a symmetry of the transfer functions has been achieved which further simplifies reflections in the coupled system.

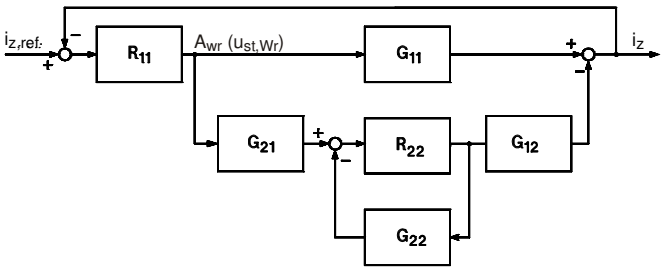

Fig. 6 Active controlled system for the DC-link current controller

The reference transfer functions of the two control circuits - which are considered as being not cross-coupled - have therefore been conformed. The desired reference transfer function for both control circuits is (symmetry condition):

$$F_W = \frac{1}{1 + 2DT_0 p + T_0^2 p^2} \quad . \tag{4}$$

With the transfer function for the excitation current controller

$$R_{22} = K_{R22} \frac{1 + pT_{R22}}{T_{R22}} \tag{5}$$

and because of the symmetry condition ($F_{W11} \approx F_{W22}$) $T_{R22} = T_f$, the following reference transfer function is achieved for the excitation current control circuit:

$$F_{W22} = \frac{K_{22} K_{R22} (1 + pT_f)}{(1 + pT_{gr})(1 + pT_{G1}) pT_f + K_{22} K_{R22} (1 + pT_f)} \tag{6}$$

A first order low pass filter series-connected to the controller has been taken into account in the transfer function which is meant to keep away interspersed failures from the controller entry. With the approaches $K_{22}K_R \gg 1$, $K_{22}K_RT_f + T_f \approx K_{22}K_RT_f + T_{gr} + T$ und $T_{gr}T \ll (T_{gr} + T)T_f$ the following applies:

$$F_{W22} = \frac{K_{22} K_{R22}}{K_{22} K_{R22} + (T_{gr} + T) p + T_{gr} T p^2}$$

$$mit\ T_0^2 = \frac{TT_{gr}}{K_{22} K_{R22}}\ ,\quad D = \frac{1}{2} \frac{T_{gr} + T}{\sqrt{TT_{gr} K_{22} K_{R22}}}\ , \tag{7}$$

$$T = T_{G1} + T_t \quad \Rightarrow K_{R22} = \frac{(T_{gr} + T)^2}{4D^2 T_{gr} T K_{22}} \quad .$$

$$R_{11} = K_{R11}^* \frac{1 + pT_{k1}}{T_f p (1 + pT_{ce})} = K_{R11} \frac{1 + pT_{k1}}{pT_{k1} (1 + pT_{ce})} \tag{8}$$

For the DC link current control circuit emerges with the controller transfer function
and with the transfer function of the lowpass filter also series-connected to this controller

$$F_{G1} = \frac{1}{1 + pT_{G1}} \tag{9}$$

with the same approaches as with the reference transfer function:

$$F_{W_{11}} = \frac{K_{11} K_{R11}^*}{K_{11} K_{R11}^* + (T_{gr} + T_{G1}) p + T_{gr} T_{G1} p^2}$$

$$mit\ T_0^2 = \frac{T_{G1} T_{gr}}{K_{R11}^* K_{11}}\ ;\quad D = \frac{1}{2} \frac{T_{gr} + T_{G1}}{\sqrt{T_{G1} T_{gr} K_{R11} K_{11}}} \tag{10}$$

$$\Rightarrow K_{R11}^* = \frac{(T_{gr} + T_{G1})^2}{4D^2 T_{gr} T_{G1} K_{11}};\ K_{R11} = K_{R11}^* \frac{T_{k1}}{T_f}\ ;\ T_{R11} = T_{k1}.$$

The controller layout in accordance with the mentioned symmetry condition led to the desired symmetry of the reference transfer function of the main controlled system. When the cross-coupled two-variables control system (see fig. 5) is taken into consideration and a controller is used as determined in advance by the a.m. calculations, a full symmetry is obtained for the main control systems in this case, too which does not only include the pole points of the main control systems but also pole and zero points originating from the cross-coupling systems.

This following characteristic polynomial emerges for the closed control circuits:

$$1 - \frac{G_{21} G_{12}}{G_{22} G_{11}} \frac{R_{22} G_{22}}{1 + R_{22} G_{22}} \frac{R_{11} G_{11}}{1 + R_{11} G_{11}} = 0 \quad . \tag{11}$$

If both controllers are laid out for the same damping D = 1, the following clear equation is obtained:

$$1 - v_K \frac{T_f p}{(1 + T_f p)(1 + T_{k1} p)} \frac{1}{(1 + T_E p)^4} = 0$$

$$mit\ T_E = \sqrt{\frac{T_{gr} T_{G1}}{K_{R11}^* K_{11}}} = \sqrt{\frac{T_{gr} T_{G1}}{K_{R22} K_{22}}}\ ;\quad v_K = \frac{K_{11} K_{21}}{K_{11} K_{22}}\ . \tag{12}$$

This special characteristic equation is simultaneously applicable to a single-loop equivalent system (see Fig. 8). According to Mückli [4], the equivalent system features the same properties as the examined two-variables control.

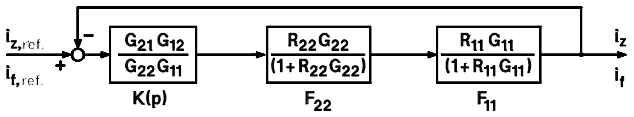

Fig. 7 Block diagram of the single-loop equivalent control circuit for the internal two-variables control

The coupling factor K(p) contains the transfer functions of the cross-coupling systems so that it offers a suitable approach for the classification of two-variables systems. It contains a mere D-proportion so that the static coupling factor becomes zero. Consequently, the examination is confined to the dynamic portion of the coupling factor.

The system becomes instable when $|K(j\omega)|$ is higher than one [4]. An asymptotic stability arises for the examined system when the gain of the coupling factor v_K is equal to one. The two-variables control system is stable for all operating states when v_K is smaller than one over the entire frequency range.

Of particular importance is the fact that this stability criterion is independent of the controller setting, when the two controllers - with main systems assumed as being uncoupled for the layout - form separate control systems. Parameter fluctuations of the controlled systems during operation of the plant also change the reference transfer functions of the main control circuits considered as being uncoupled, so that it was possible to approach the equivalent time constants in the a.m. manner. The stability of the coupled system is not affected by the controller layout.

Fig. 8 shows the simulation results for the coupled two-variables control system. When the controller parameters are laid out in accordance with the symmetry condition, both control circuits feature, as expected, the same reference and disturbance behaviour, whereby reference and disturbance behaviour themselves are either characterised by a comparable control quality. Therefore, the internal two-variables control method provides the desired excellent reference behaviour and a low mutual interacting of the control circuits.

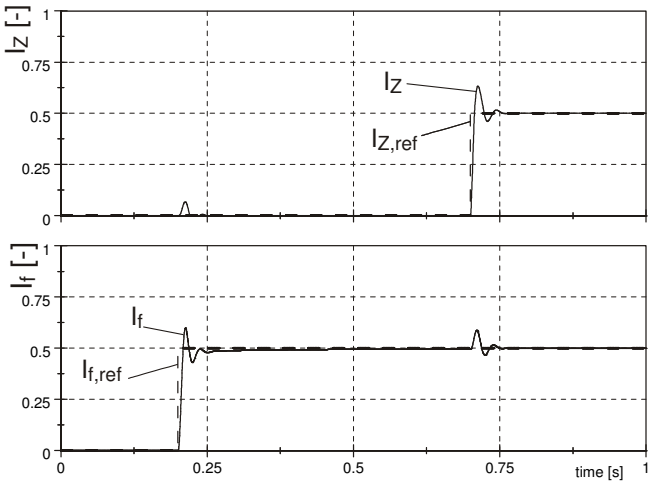

Fig. 8 Step response of the internal two-variables control system; a) according to the symmetry condition, b) amount optimum, c) symmetrical optimum

B. Inverter rest position controller

The inverter position controller means a further intermeshing of the internal two-variables control system (see Figs. 1 and 9). At the same time, it supplies the rated value for the excitation current controller so that it is inapplicable as an external system entry. The rated value for the inverter position controller is adjusted to a fixed value which corresponds to a control factor of $A_{Wr0} = 0.9$ at the inverter. By linearisation of the system at its operating point and the associated system analysis in the small signalling range, the rated value becomes zero for the inverter position controller.

Due to the reduction to one input variable, the number of important reference transfer functions is reduced to two (B_{11}, B_{21}). The two transfer functions feature identical denominator polynomials but different numerators.

Now the characteristic system equation reads:

$$1+\frac{(G_{GI}R_{WL}-G_{21})\,G_{12}}{G_{11}G_{22}}\;\frac{R_{22}G_{22}}{1+R_{22}G_{22}}\;\frac{R_{22}G_{22}}{1+R_{11}G_{11}}=0\ . \quad \textbf{(13)}$$

The characteristic equation shows that with the transfer function R_{WL} the effect of the coupled system G_{21} can be changed by the inverter position controller. This has a further stabilization effect on the system, if applicable. Following relation emerges for the transfer function of the modified coupled system with $T_{G1} = T_{kl}$ (fig. 10):

$$\frac{T_{RWL}p^2(K_{RWL}T_{gr}-K_{21})+(T_{gr}+T_{RWL})K_{RWL}p+K_{RWL}}{T_{RWL}p\,(1+T_{gr}p)\,(1+T_{kl}p)}=-G_{21}^{*} \qquad \textbf{(14)}$$

In order to make the modified coupled transfer function G^{*}_{21} as simple as possible, the highest numerator power has been eliminated by a suitably chosen K_{RWL} .

$$K_{RWL}=\frac{K_{21}}{T_{gr}}\ ;\quad (T_{gr}\ in\ [s]) \qquad \textbf{(15)}$$

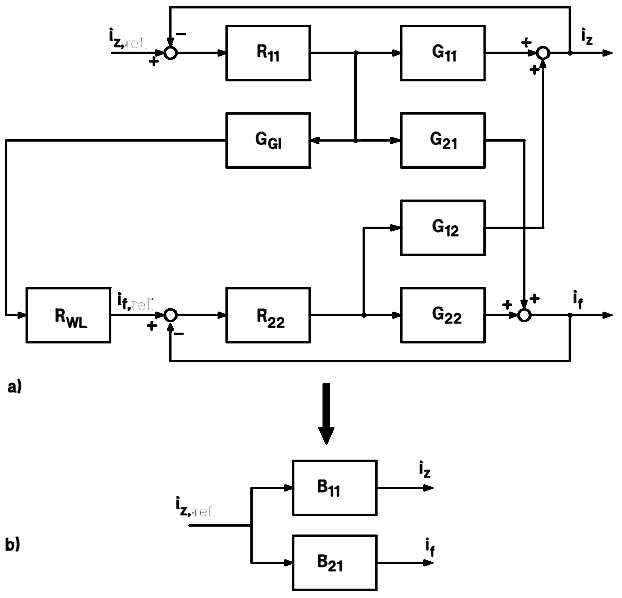

Fig. 9 Inverter rest position control

One problem with this controller setting is that a change of $K_{21}=T_D$ during operation may also happen at higher values so that a higher controller gain would be necessary for compensation. If no adaptive controller is used, not only a further zero point would arise but it could also contain a positive real part.

High closed-loop gains may cause a system instability. After compensation of the highest numerator power follows:

$$K_{21}\,\frac{(T_{gr}+T_{RWL})\,p+1}{T_{gr}T_{RWL}\,p\,(1+T_{gr}p)\,(1+T_{kl}\,p)} = -G^{*}_{21}\ . \qquad (16)$$

The original DT_2-element (G21) is converted into an IT_2-element ($-G^{*}_{21}$) by the inverter rest position controller. Consequently, the characteristic reference transfer function equation reads as follows (see equ. (12)):

$$1+v_K\,\frac{1+p\,(T_{gr}+T_{RWL})}{(1+pT_{kl})\,(1+pT_f)\,p}\;\frac{1}{(1+pT_{Ers})^4}=0 \qquad (17)$$

$$mit\ v_K=\frac{K_{12}K_{21}}{K_{11}K_{22}T_{gr}T_{RWL}}\ .$$

A determination of the time constant T_{RWL} must be carried out iteratively since it affects the zero point as well as the gain v_K of the characteristic equation. Fig. 10 shows the step response on the test facility of the controlled system which consists of internal two-variables control and an inverter position control. The set-value step function from 0.15 to 0.6 corresponds to a change of the DC-link current of 6A to 18A in a real system.

The step response shows a high dynamic of dc-link current control loop. In the time curves are not any influences between the i_z- and the i_f-control loop visible. This means a decoupling of the both control loops is successfully realized.

In the first phase of the control procedure the dc-link current is set to the reference by increase of the inverter control factor $A_{wr.}$ After the control factor is led back to the rest position by increase the excitation current. As a result the amplitude of manipulated variable of the inverter A_{Wr} is available for the next dynamic control procedure in both directions.

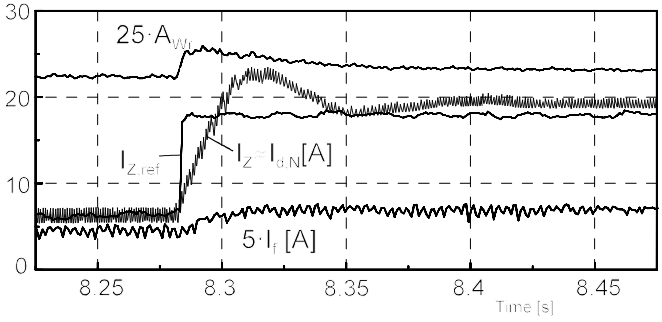

Fig. 10 Step response of control circuit with inverter rest position controller; values at the test bench

V. Conclusion

The realized basic control concept meets the requirements to a large extent so that the conditions are provided for operation at maximal power coefficient c_{Pmax} of the wind rotor over a wide range of wind speeds. In addition, the operation within a wide speed range $(0{,}6 \ldots 1{,}2)f_N/p$ makes it also possible to utilize the rotating masses for energy storage. This offers the basis to smooth short-term wind-bound power fluctuations by suitable power control methods.

On the other hand, the control concept is characterised by sufficiently high control dynamics. The inverter as control element allows for the damping of low-frequent current beats in the DC-link circuit.

Besides sufficiently high control reserves for an operation within a broad speed range and high control dynamics, a stable operation over the whole speed range has been obtained for the controller by means of the layout criteria. An insensitivity of the control concept to parameters voids comprehensive controller realizations like e.g. parameter-adaptive controllers.

References

[1] C. Sourkounis, "Windenergiekonverter mit maximaler Energieausbeute am leistungsschwachen Netz", Dissertation, Papierflieger Clausthal 1994

[2] H. Bühler, "Einführung in die Theorie geregelter Drehstromantriebe", Band 1, 2, Birkhäuser Verlag Basel 1977

[3] J. Leimburger, "Untersuchung des statischen und dynamischen Verhaltens drehzahlgeregelter Stromrichter-Synchronmotoren unter Berücksichtigung verschiedener Regelverfahren.", Dissertation 1977

[4] W. Mückli, "Analyse und Optimierung nicht entkoppelter Zweifachregelkreise" Dissertation Aachen 1968

[5] Ni, B.; Sourkounis, C.; "Investigations on Control Methods for Variable Speed Wind Energy Converters at Strongly Fluctuating Wind Power", 34th Annual Conference of the IEEE Industrial Electronics Society, IECON 2008, 10-13 November 2008 in Orlando, Florida, USA

[6] C. Sourkounis and B. Ni, "Optimal control structure to reduce the cumulative load in the drive train of wind energy converters," 11th European Conference on Power Electronics and Applications, Dresden, Germany

[7] F. Hughes, O. Anaya-Lara, N. Jenkins, and G. Strbac, "Control of DFIGbased wind generation for power network support," IEEE Transactions on Power Systems, vol. 20, no. 4, 2005

[8] Xibo Yuan; Wang, F.; Burgos, R.; Yongdong Li; Boroyevich, D.; , "Dc-link voltage control of full power converter for wind generator operating in weak grid systems," Applied Power Electronics Conference and Exposition, 2008. APEC 2008. Twenty-Third Annual IEEE , vol., no., pp.761-767, 24-28 Feb. 2008

Symbols

A_{Wr} : control factor of the inverter
C : capacity
c_{Pmax}: max. Power coefficient of wind rotor
D : damping
f : frequency
i : standardized current
I : effective current value
i(t) : instantaneous value of the current
L : inductance
I_{1L} : actual value of the first harmonic
L_{KM} : generator-side commutation inductivity
L_{KN} : lineside commutation inductivity
m_R : rotor torque (standardized)
m_{el} : generator counter-torque (standardized)
n_G : generator speed
P : active power
P_z : electrical effective power output (electric power in the DC-link)

P_R : power realized by the wind rotor
Q : reactive power
r : standardized resistance
R : ohmic resistance
S : apparent power
T : time constant
T_m : mechanical time constant
T_{gr} : high equivalent time constant of the controlled system
T_{kl} : small equivalent time constant of the controlled system
T_z : DC-link time constant
T_f : excitation current time constant
T_t : delay time constant of the line-commutated rectifier
$u_{st,f}$: standardized control voltage of the field current rectifier
$u_{st,Wr}$: standardized control voltage of the inverter
u : standardized voltage
U : effective voltage value
u(t) : instantaneous value of the voltage
w : wind speed
z : standardized impedance

α : control angle
α_u : overlap angle
φ_{sM} : phase displacement between phase voltage and current of generator
$\varphi_1{}^1$: first harmonic phase displacement between phase voltage and current of generator
ω : angular speed

Indices
d : quantities in the longitudinal axis of the synchronous machine (d-q-system)
D : quantities in the damper winding of lingitudinal axis
f : quantities of excitation winding of the synchronous machine
f0 : quantities of excitation winding for idle running of the synchronous machine
Gr : rectifier quantity
K : commutation quantity
L : conductor quantity
M : machine quantity
N : grid quantity
nen : rated quantity
q : quantity in the transverse axis of the synchronous machine (d-q-system)
Q : damper winding in the transverse axis
s : phase quantity
S : stator quantity
Wr : inverter quantity
z : DC-link quantities